Physics of Size Selectivity

Roland Roth[1,2] and Dirk Gillespie[3]

[1]Max-Planck-Institut für Metallforschung, Heisenbergstrasse 3, D-70569 Stuttgart, Germany
[2]ITAP, Universität Stuttgart, Pfaffenwaldring 57, D-70569 Stuttgart, Germany
[3]Department of Molecular Biophysics and Physiology, Rush University Medical Center, Chicago, Illinois 60612, USA

(Received 11 March 2005; published 9 December 2005)

We demonstrate that two mechanisms used by biological ion channels to select particles by size are driven by entropy. With uncharged particles in an infinite cylinder, we show that a channel that attracts particles is small-particle selective and that a channel that repels water from the wall is large-particle selective. Comparing against the extensive density-functional theory calculations of our model, we find that the main physics can be understood with surprisingly simple bulk models that neglect the confining geometry of the channel completely.

DOI: 10.1103/PhysRevLett.95.247801 PACS numbers: 61.20.−p, 87.15.−v, 87.16.Uv

Ion channels are membrane-spanning proteins that passively transport ions down their electrochemical gradients. Channels can open and close their pores upon stimulation, a process called gating. In addition, some channel types can preferentially select the ion species they conduct. These properties make channels responsible for a large number of physiological phenomena, including propagating action potentials along neurons and initiating muscle contraction. Experimentally, channels can be studied either *in vivo* or in well controlled but nonphysiological conditions one channel at a time [1].

Experimentally, eleven ''selectivity sequences'' have been found that rank the relative preference of a channel for conducting alkali metal ions through cation channels [1]. In this Letter, we focus on the two extreme selectivity sequences where the channel prefers to conduct small ions or large ions. Examples of small-alkali metal cation selective channels include the *L*-type calcium channel, the ryanodine receptor (RyR), and the neuronal sodium channel. Examples of large-ion selective channels include voltage-gated potassium channels, gramicidin A (gA), and the nicotinic acetyl choline receptor (nAchR).

All channel pores are several nanometers in length and have radii ranging from approximately 2 Å for gA and potassium channels to >5 Å for porin channels and nAchR. Although its dimensions are small and similar to the size of ions, equilibrium bulk models for selectivity [2–4] that neglect confining due to the pore can help to *understand* experiments [2] and reproduce results from Monte Carlo simulations qualitatively [5]. These and other studies of selectivity [6–9] found that highly charged channels such as the sodium, *L*-type calcium and RyR channels are small-ion selective because smaller ions neutralize the charge on the protein in a smaller volume, a mechanism named charge-space competition. For large-ion selectivity, there are several theories, some based on the dehydration energy of ions [1,10] and others based on the repulsion of water from hydrophobic regions of the channel, without explicit ion hydration [4].

In the present Letter, we wish to extend the understanding of the physical mechanism that underlies size selectivity by highlighting entropy as a driving force in both selectivity mechanisms. To do so, we choose a model with the smallest number of parameters that allows one to study the phenomenon of size selectivity. This model consists of a mixture of uncharged hard spheres with different radii [11]. This model obviously neglects electrostatics as well as effects caused by hydration shells. In our model, the hard-sphere ''cations'' are attracted into and the hard-sphere ''anions'' are repelled from the selectivity filter through an *effective* potential, which parametrizes the long-ranged contribution such as the Donnan potential. We denote its amplitude by $U_{\mathrm{attr}} > 0$. We have verified that, due to the mentioned repulsion, the presence of anions in the system has a very small effect on the results. For the sake of simplicity, we therefore include only the solvent and hard-sphere cations in our model. For studying large-ion selective channels such as the gA channel, we introduce an effective repulsion $V_{\mathrm{rep}} > 0$, which models the hydrophobic repulsion of water from the channel.

Here we focus on the importance of the entropy of both the ions and the solvent, which is often neglected in models of biological systems. Our approach is in line with the findings of theoretical studies of biological problems in different areas such as protein folding [12]. If the solvent is modeled as a fluid of particles with a size comparable to that of the other species, it provides a crowded environment for the ions, which in turn have to compete for free space even at low ion concentrations. U_{attr} and V_{rep}, the amplitudes of the ion attraction and the water repulsion, respectively, are simply parameters in our model. Since we wish to understand the *phenomenon* of size selectivity among equally charged ions, a detailed account of electrostatic and hydrophobic interactions will modify the selectivity of the channel quantitatively but not the role of entropic forces described here.

In order to test if such a simple system selects particles by size, we start by considering two compartments. The

bath, denoted compartment I, contains ions at given concentrations of the order of 100 mM dissolved in a crowded solvent of 55.5 M, the density of pure water under normal conditions. A second compartment, denoted compartment II, models either the selectivity filter of the channel that attracts ions by the action of U_{attr} or a hydrophobic channel that repels water by the action of V_{rep}. Inhomogeneities caused by the confining geometry of the protein are ignored at this stage but are included later in our density-functional theory (DFT) calculations.

By allowing equilibrium between the compartments, the concentration of all components in the filter adjust so that the grand potential of the system is minimized. This is described by the equality of the chemical potential $\mu_i^\alpha = \partial f(\{\rho_j^\alpha\})/\partial\rho_i$ of species i between compartments $\alpha =$ I, II, where ρ_i^α is the corresponding number density of this component. For the free energy density of the mixture f, we employ the expression corresponding to the Mansoori, Carnahan, Starling, and Leland (MCSL) [13] equation of state. For the ion components, we obtain

$$\mu_i^{\text{I}}(\{\rho_j^{\text{I}}\}) = \mu_i^{\text{II}}(\{\rho_j^{\text{II}}\}) + U_{\text{attr}}, \tag{1}$$

and for the water component

$$\mu_{\text{H}_2\text{O}}^{\text{I}}(\{\rho_j^{\text{I}}\}) = \mu_{\text{H}_2\text{O}}^{\text{II}}(\{\rho_j^{\text{II}}\}) - V_{\text{rep}}. \tag{2}$$

U_{attr} and V_{rep} are the electrostatic and hydrophobic parts of the chemical potential. Equations (1) and (2) are coupled, highly nonlinear equations that determine the densities in the filter compartment ρ_i^{II} for given densities in the bath ρ_i^{I} and parameters U_{attr} and V_{rep}. This bulk model allows us to study the physics of size selectivity assuming that inhomogeneities in the pore are unimportant. In order to quantify which component is preferentially absorbed in the pore, we define the absorbance of component i, $\xi_i \equiv \rho_i^{\text{II}}/\rho_i^{\text{I}}$, which compares the density of component i in the filter to that in the bath. The selectivity $S_{i,j}$ of the filter is defined by $S_{i,j} \equiv \xi_i/\xi_j$.

The assumption that the inhomogeneities are not important can be tested by taking the confining geometry of the pore into account within the framework of DFT. Here we employ a recently improved version of Rosenfeld's fundamental measure theory which is based on the accurate MCSL equation of state [14]. In addition to the inputs to our bulk model, the DFT approach also requires a model for the protein that forms the pore of the selectivity filter. The simplest way to incorporate the effect of the protein in the DFT approach would be to define external potentials $V_i^{\text{ext}}(\mathbf{r})$ that confine particles of all components inside the channel. Unfortunately, the actual form of $V_i^{\text{ext}}(\mathbf{r})$ is unknown because of the unknown structure and mechanical properties of the protein. In our study, we choose to model the protein as a hard-sphere fluid which is restricted by a hard-wall potential to a region *outside* the pore. If the "protein fluid" is sufficiently dense, spheres of other components will find it difficult to enter the protein. In this way, the protein fluid acts as a rough wall that can be penetrated by particles of other components, which is more appropriate than a smooth, hard wall. We model the pore as an infinitely long cylinder, which simplifies the calculations because the density profiles $\rho_i(\mathbf{r}) = \rho_i(r)$ of all components, labeled by i, depend only on the radial distance r.

By minimizing the density functional of a N-component mixture $\Omega[\{\rho_i(\mathbf{r})\}]$, we obtain the inhomogeneous equilibrium density profiles $\rho_i(r)$, as well as the grand potential Ω of the system. From these, we derive all quantities of interest. As mentioned above, we consider an external potential acting only on the protein component, which in turn acts on the other components in the pore so that they develop inhomogeneous structures. If we take the limit of the protein fluid density going to zero, no external potential acts on the system and we recover our bulk approach. In addition to the parameters entering our bulk approach, two new parameters are required to describe the system fully, namely, the protein fluid packing fraction η_p and the pore radius R_{pore}, which defines the region $r < R_{\text{pore}}$ from which the protein fluid is expelled. Here we chose $\eta_p = 0.45$ and the diameter of the particles that constitute the protein to be 2.45 Å.

In our DFT calculations, we obtain the absorbance of species i inside the pore from its density profile $\rho_i(r)$ by

$$\xi_i = \frac{2}{\rho_i^{\text{I}} R_{\text{pore}}^2} \int_0^{R_{\text{pore}}} dr r \rho_i(r). \tag{3}$$

If the inhomogeneities in $\rho_i(r)$ are small, this definition yields numbers for the absorbance and the selectivity very close to those predicted by the bulk approach.

We start by reporting results of our bulk approach which highlight the role of competition between ion species for free volume in the filter. We consider a bath consisting of a binary mixture of 100 mM Na *or* 100 mM K in water and attract ions into the filter by the potential U_{attr}, in the range from 0 to $10k_BT$. As a result of the attraction, the concentration of Na or K in the filter increases. We quantify the effect of the attractive potential by the absorbance ξ_i, $i =$ Na, K, and show its dependence on U_{attr} in Fig. 1. The dotted line in Fig. 1 shows the result for the binary mixture of Na and water, obtained by the bulk approach, and the dashed-dotted line shows the corresponding quantity for the binary mixture of K and water. Comparing these results, we observe a similar increase in the filter compartment for both species, especially at small values of U_{attr}, because in that regime the particles still find free space between the solvent particles. At higher values of U_{attr}, however, Na must squeeze out less water from the filter than K to follow the attraction, because $\sigma_{\text{Na}} < \sigma_{\text{K}}$. The result is that $\xi_{\text{Na}} > \xi_{\text{K}}$ and, hence, the selectivity $S_{\text{Na,K}} = \xi_{\text{Na}}/\xi_{\text{K}} > 1$, as is shown in the inset in Fig. 1 (dotted line). An attractive channel favors smaller species. In this case, there is no direct competition between species of different size and the selectivity $S_{\text{Na,K}}$ remains small, leveling off at 2.2 for large values of U_{attr}.

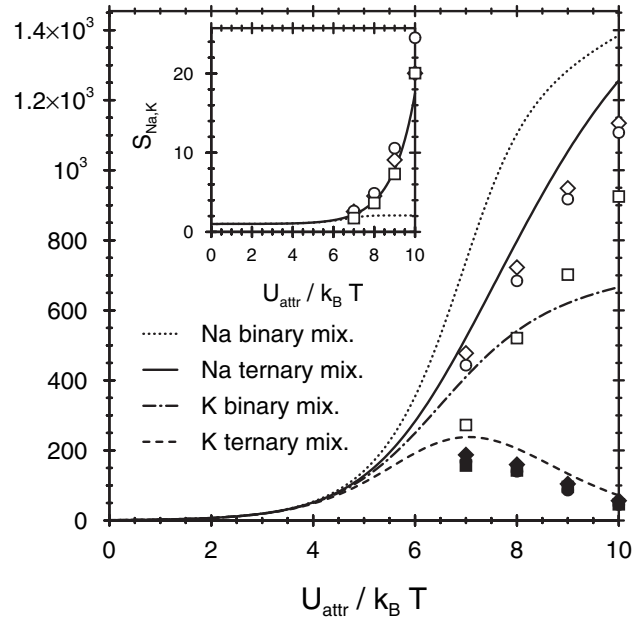

FIG. 1. The absorbance ξ_i of Na and K in an attractive filter as a function of U_{attr}. We compare bulk results (lines) for a binary mixture to those for a ternary mixture. In the ternary mixture of water, Na, and K, the competition for space leads to a selectivity of the smaller component, $S_{\text{Na,K}} \gg 1$, as is shown by the solid line in the inset. The symbols, which are explained in the text, denote DFT results for the ternary case.

The situation becomes much more interesting and richer if we consider a ternary mixture of water, 100 mM Na, *and* 100 mM K in the bath. Both ion species feel the attraction and are in direct competition for the free volume in the filter. The result of this competition, within the bulk approach, can be seen in Fig. 1 (solid and dashed lines). For weak attractions, the situation is similar to the previous system; i.e., the ions fill the free volume between solvent particles and the actual size of the ions is unimportant. At stronger attractions, however, when the ions no longer find free volume, they have to squeeze water out of the filter to follow the attraction. When the water concentration in the filter is significantly reduced, direct competition between the ion species sets in, and it becomes energetically and entropically more favorable for the system to allow the smaller ion species to fill the volume by squeezing out the larger ions. The Na concentration in the filter continues to increase, while the K concentration starts to decrease. If the attraction is sufficiently strong, this effect can be dramatic and results in a large selectivity $S_{\text{Na,K}} \gg 1$, as we show in the inset in Fig. 1 (solid line). It is important to realize that this physical mechanism always prefers the smallest ion species and prefers Li over Na if we were to start with a bath consisting of water, Li, and Na.

We test the predictions of our bulk approach by extensive DFT calculations of our model by changing the pore radius R_{pore} from 1 to 5 Å. Some DFT results for $R_{\text{pore}} =$ 2.1 Å (squares), 3.5 Å (circles), and 5 Å (diamonds) are shown in Fig. 1 and its inset. Solid and open symbols denote results for K and Na, respectively. We find that, if the pore is sufficiently wide, the DFT results for the selectivity are in good agreement with our bulk predictions, although the absorbances obtained from DFT deviate slightly from the corresponding bulk values. This agreement indicates that in this case the inhomogeneities caused by the confinement are moderate. Most channels whose radii are known have radii $\geq$3 Å [1,8,9]. If, however, the pore radius becomes smaller ($\lesssim$2.5 Å) and nearly equal to the particle radii, the confinement becomes increasingly important and results in deviations between DFT and bulk results. In this regime, we observe nonlinear absorbance behavior similar to that described by Goulding *et al.* [15]. In narrow attractive channels, the small-ion selectivity can be increased dramatically. Channels known to have radii this small include gA [1] and the KcsA potassium channel [10].

A set of density profiles of the Na and K species for various values of U_{attr} is shown in Fig. 2. The pore radius is $R_{\text{pore}} = 3.5$ Å, and the ion concentrations in the bath are $\rho_{\text{Na}} = \rho_{\text{K}} = 100$ mM. These profiles demonstrate the monotonic increase of Na and the nonmonotonic behavior of K in the pore as U_{attr} is increased. We find that the structures in the density distributions of the ions follow closely the densities predicted by the bulk approach.

Now we turn to a different type of channel that is characterized by hydrophobic protein walls, which we take into account by the effective water repulsion V_{rep}. Weakly charged channels such as gA and nAchR seem to have these properties (Ref. [4], and references therein). The little charge in these channels is sufficient to repel anions from the channel but not to distinguish between

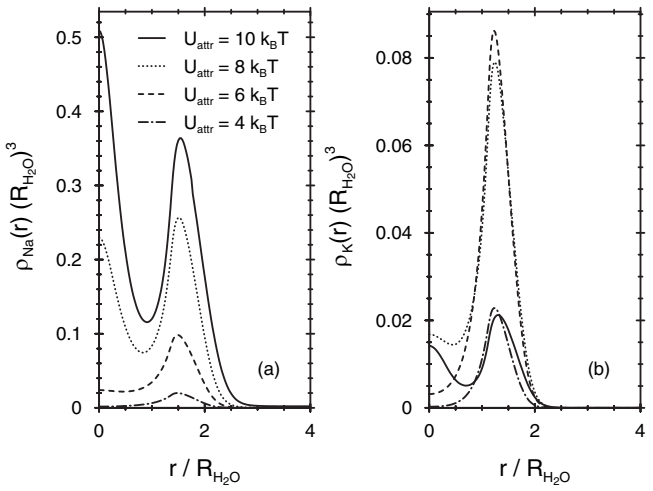

FIG. 2. Typical density distributions of (a) Na and (b) K inside an attractive, cylindrical filter as obtained from DFT for various values of U_{attr}. r denotes the radial coordinate. While the density of (a) Na increases monotonically with U_{attr}, the density of (b) K shows a nonmonotonic behavior. For the radius of water, we use $R_{\text{H}_2\text{O}} = \sigma_{\text{H}_2\text{O}}/2 = 1.4$ Å [11].

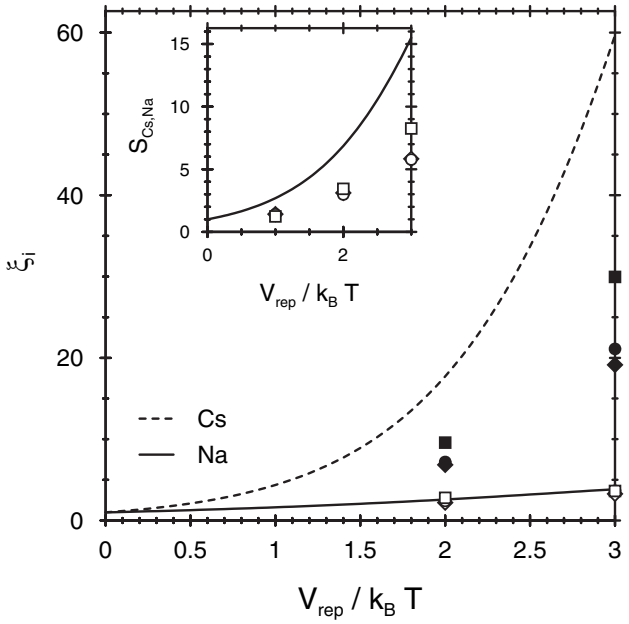

FIG. 3. The absorbance ξ_i of Cs and Na in a hydrophobic filter as a function of V_{rep}. With increasing value of V_{rep}, both ion densities increase; however, the density of the larger component increases faster. The selectivity of Cs over Na is shown in the inset. Lines denote bulk results, while symbols, which are explained in the text, denote those obtained by DFT.

cations of different size. In order to keep our model as simple as possible, we neglect the anions and set $U_{\text{attr}} \equiv 0$; however, we have verified that an extended model that includes a weak cation attraction and hard-sphere anions which are repelled from the channel predict equivalent results. Following Ref. [4], we consider $V_{\text{rep}} \leq 3k_BT$. In the present study, we compare 100 mM of both Na and Cs, which have a more pronounced size difference than Na and K [11], considered earlier.

In Fig. 3, we show the absorbance of Na (solid line) and Cs (dashed line) in a hydrophobic pore as a function of V_{rep} for a ternary mixture with $\rho_{\text{Na}} = \rho_{\text{Cs}} = 100$ mM, predicted by the bulk theory (lines) and the corresponding selectivity $S_{\text{Cs,Na}}$ in the inset. While the densities of both species increase monotonically as the water repulsion increases, the density of the larger component, Cs, increases faster than that of the smaller component, Na. Hence, the channel is large-ion selective.

Again we test the prediction of the bulk approach by DFT calculations. In order to account for the hydrophobic interaction between the protein and water, we introduce an external potential acting on the water. $V^{\text{ext}}_{\text{H}_2\text{O}}(r)$ repels water only from a 1.4 Å neighborhood of the protein. This is a clear difference between the DFT and the bulk approach, which by construction cannot take surface effects into account. This difference is reflected by lower Cs densities in the pore obtained from DFT (symbols) as compared to the bulk theory (lines) in Fig. 3 and the smaller selectivity in the inset in Fig. 3. Here the squares, circles, and diamonds denote DFT results for $R_{\text{pore}} = 2.8$, 3.5, and 5 Å, respectively. This difference gets smaller as the radius of the pore is reduced. The overall agreement is still qualitatively good.

Our extensive DFT study confirms the validity of the bulk approach for both kinds of channels also for different choices for η_p and ion concentrations. The confining geometry of the pore becomes important only if the radius of the pore is comparable to the radii of particles inside the pore. Our findings also show clearly that the entropy of the mixture of particles is enough to give size selectivity and, hence, has to be taken into account properly. A very important, yet often neglected, contribution to this entropy stems from the fact that water is a dense fluid and leaves little space to the ions.

R. R. thanks R. S. Eisenberg for his hospitality and stimulating discussion during his stay in Chicago and R. Evans for helpful comments on the manuscript. D. G. is grateful for support of the HIH Grant No. GM 067241 (Principal Investigator Bob Eisenberg).

[1] B. Hille, *Ion Channels of Excitable Membranes* (Sinauer Associates, Sunderland, MA, 2001).
[2] W. Nonner, L. Catacuzzeno, and B. Eisenberg, Biophys. J. **79**, 1976 (2000).
[3] W. Nonner, D. Gillespie, D. Henderson, and B. Eisenberg, J. Phys. Chem. B **105**, 6427 (2001).
[4] D. Gillespie, W. Nonner, D. Henderson, and R. S. Eisenberg, Phys. Chem. Chem. Phys. **4**, 4763 (2002).
[5] See, e.g., D. Boda, D. Henderson, D. D. Busath, and S. Sokołowski, J. Phys. Chem. B **104**, 8903 (2000).
[6] D. Boda, D. D. Busath, B. Eisenberg, D. Henderson, and W. Nonner, Phys. Chem. Chem. Phys. **4**, 5154 (2002).
[7] D. Gillespie, W. Nonner, and R. S. Eisenberg, J. Phys. Condens. Matter **14**, 12 129 (2002).
[8] H. Miedema, A. Meter-Arkema, J. Wierenga, J. Tang, B. Eisenberg, W. Nonner, H. Hektor, D. Gillespie, and W. Meijberg, Biophys. J. **87**, 3137 (2004).
[9] D. Gillespie, L. Xu, Y. Wang, and G. Meissner, J. Phys. Chem. B **109**, 15 598 (2005).
[10] D. A. Doyle, J. Morais Cabral, R. A. Pfuetzner, A. Kuo, J. M. Gulbis, S. L. Cohen, B. T. Chait, and R. MacKinnon, Science **280**, 69 (1998).
[11] We take the hard-sphere diameters as the unhydrated crystal diameter from R. D. Shannon and C. T. Prewitt, Acta Crystallogr. Sect. B **25**, 925 (1969) to be $\sigma_{\text{Na}} = 2.0$ Å, $\sigma_{\text{K}} = 2.7$ Å, $\sigma_{\text{Cs}} = 3.4$ Å, and $\sigma_{\text{H}_2\text{O}} = 2.8$ Å.
[12] Y. Harano and M. Kinoshita, Chem. Phys. Lett. **399**, 342 (2004).
[13] G. A. Mansoori, N. F. Carnahan, K. E. Starling, and T. W. Leland, Jr., J. Chem. Phys. **54**, 1523 (1971).
[14] Y. Rosenfeld, Phys. Rev. Lett. **63**, 980 (1989); R. Roth, R. Evans, A. Lang, and G. Kahl, J. Phys. Condens. Matter **14**, 12 063 (2002); Y.-X. Yu and J. Wu, J. Chem. Phys. **117**, 10 156 (2002).
[15] D. Goulding, J.-P. Hansen, and S. Melchionna, Phys. Rev. Lett. **85**, 1132 (2000).